Supporting Information for

Graphene-wrapped hair-derived carbon/sulfur composite for high performance lithium sulfur batteries

Mingpeng Yu,[a] Rui Li,[a] Yue Tong,[a] Yingru Li,[a] Chun Li,[a] Jong-Dal Hong,[b] and Gaoquan Shi*[a]

[a]Department of Chemistry, Tsinghua University, Beijing 100084, People's Republic of China. Fax: 86 62771149; Tel: 86 6277 3743; E-mail: gshi@tsinghua.edu.cn

[b]Department of Chemistry, Incheon National University, 406-772 Incheon, South Korea

Table S1 Summary of the initial and final discharge capacities, as well as the capacity retentions of g-C/S electrode; the capacity retentions were calculated on account of the final and maximum discharge capacities measured at each discharge rate.

Rate (C)	Initial capacity (mA h g^{-1})	Capacity after 300 cycles (mA h g^{-1})	Capacity retention (%)
0.2	1113.2	989.2	88.8
0.5	1066.1	870.3	81.6
1.0	737.8	705.3	86.9
2.0	606.7	574.2	80.2

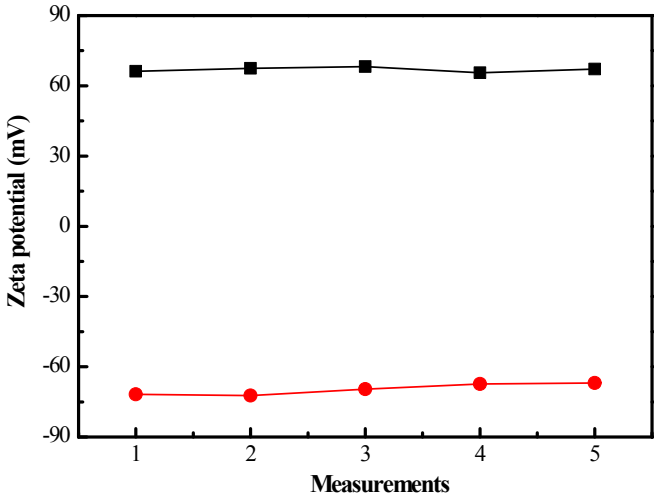

Fig. S1 Zeta potentials of the aqueous suspensions (pH ~ 5.3) of CTAB modified C/S composite (black) and graphene oxide (red); the interval of each measurement is 1.0 min.

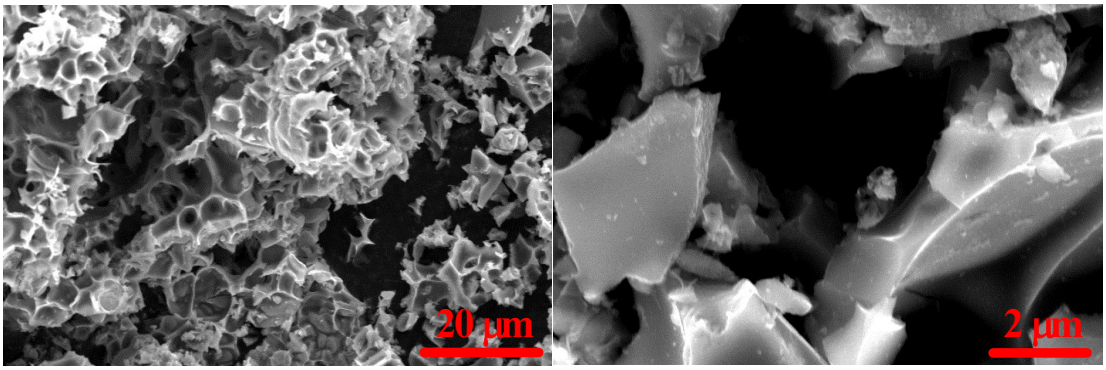

Fig. S2 SEM images of the activated carbon material prepared from hair.

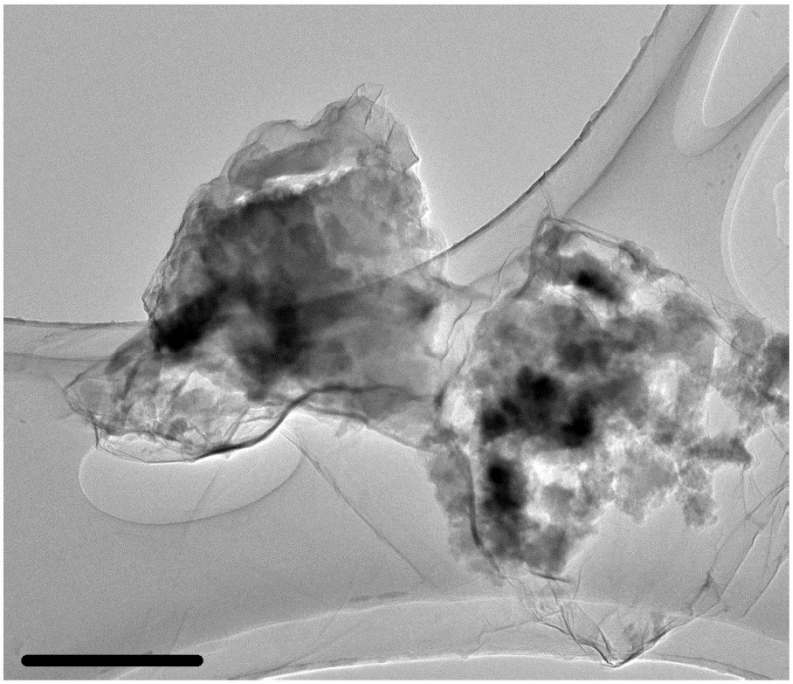

Fig. S3 STEM image of rGO wrapped C/S composite. Scale bar, 500 nm.

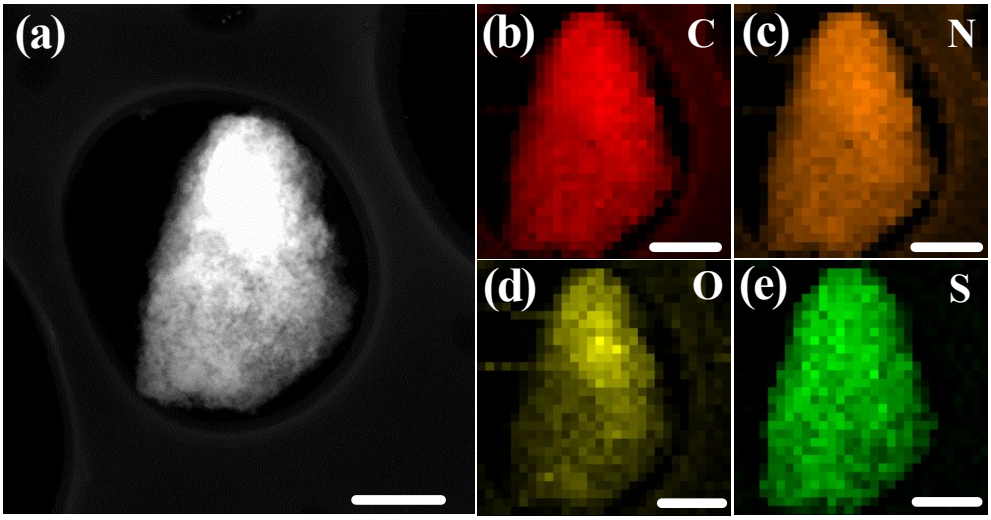

Fig. S4 (a) STEM images of C/S composite and the corresponding elemental mapping images of (b) carbon, (c) nitrogen, (d) oxygen and (e) sulfur. Scale bars, 500 nm.

Fig. S4 shows the *STEM* and the corresponding elemental mapping images *of* C/S composite. Accordingly, the C/S aggregates are composed of tiny particles because of the ball milling treatment, and they have homogeneous distributions of carbon, oxygen, nitrogen, and sulfur elements

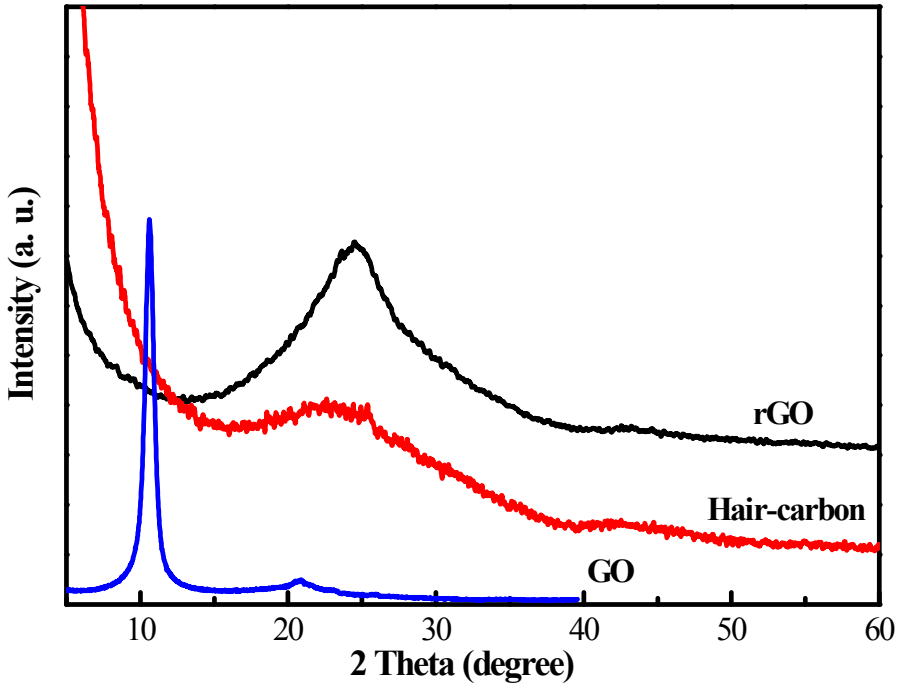

Fig. S5 XRD patterns of GO, rGO sheets and as-prepared hair carbon.

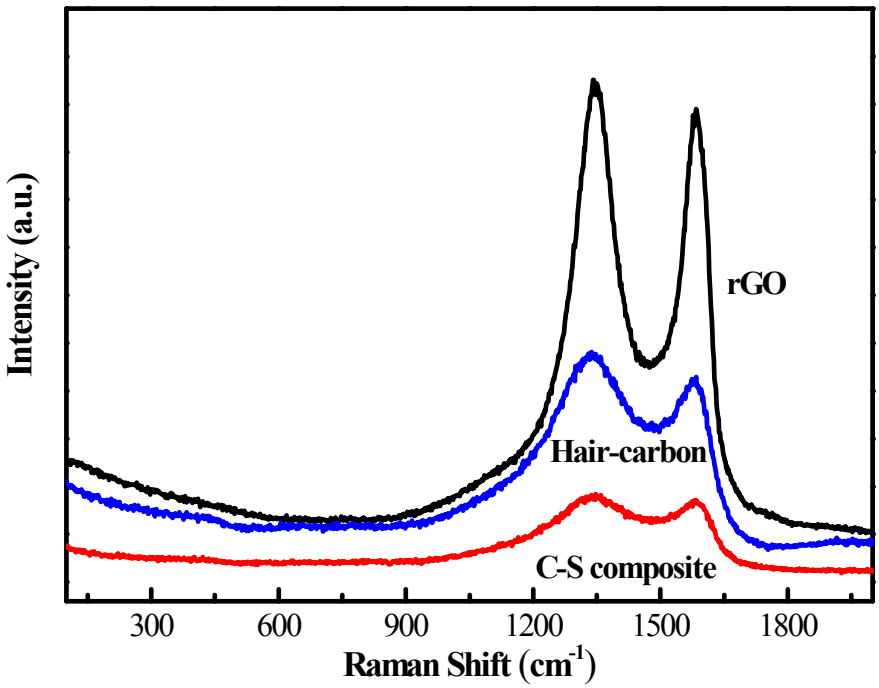

Fig. S6 Raman spectra of the rGO sheets, as-prepared hair carbon, and C/S composite.

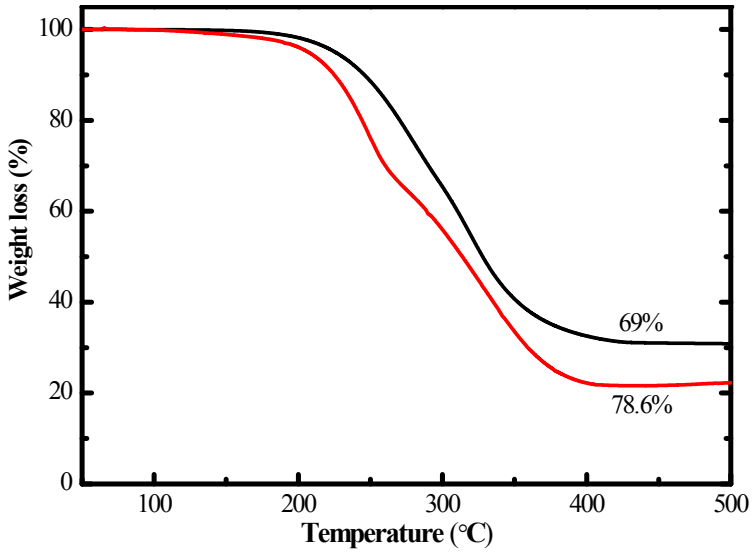

Fig. S7 TGA curves of C/S (red) and g-G/S (black) composites.

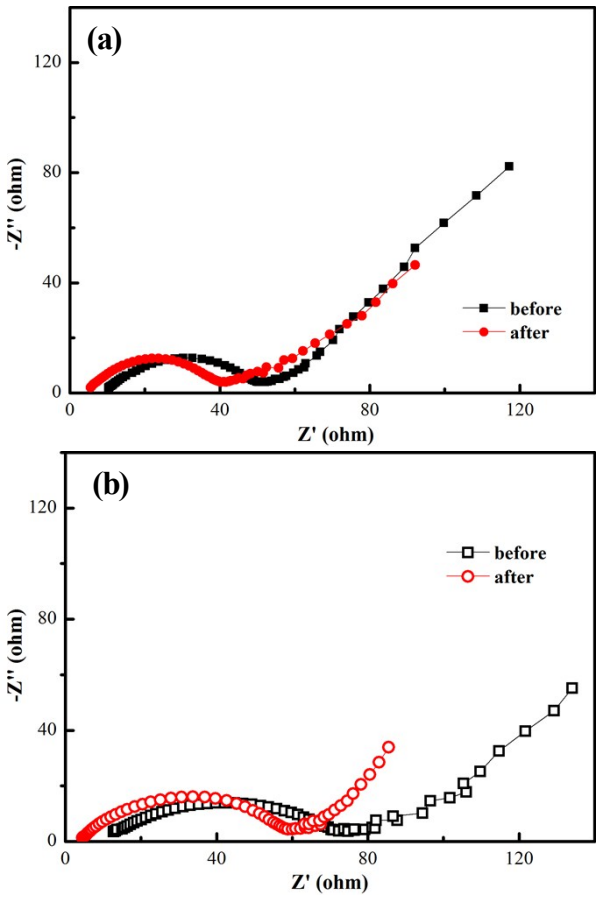

Fig. S8 Electrochemical impedance spectra of (a) g-C/S and (b) C/S electrodes before and after cycling.

The impedance spectrum of g-C/S composite electrode shows a much smaller high-frequency semicircle than that of the C/S composite electrode. Since the depressed semicircle in high frequency region is related to the contact resistance and charge transfer resistance, a smaller semicircle of g-C/S composite indicates its more efficient charge transfer process between C/S particles, attributing to the enhanced conductivity of the graphene wrapping.

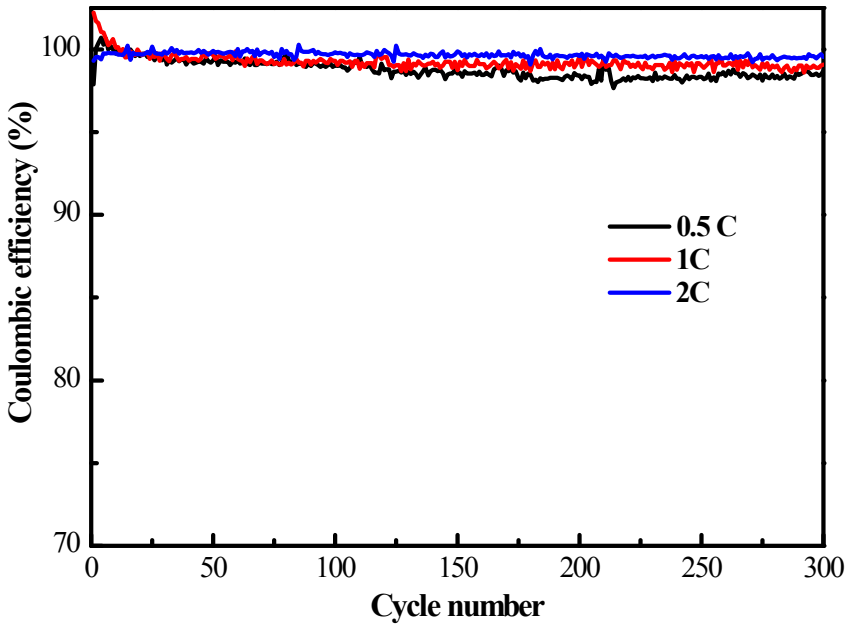

Fig. S9 Coulombic efficiencies of g-C/S composite recorded during the processes of charging/discharging for 300 cycles at different rates.

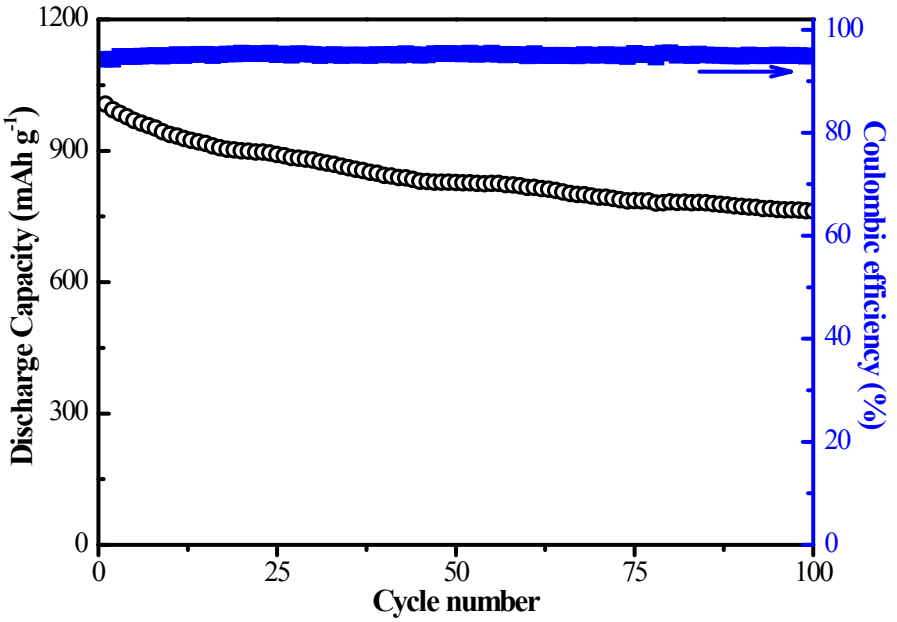

Fig. S10 Cycling performance of the g-C/S composite electrode at a constant rate of 0.2 C without $LiNO_3$ additive. The coulombic efficiency is also shown.

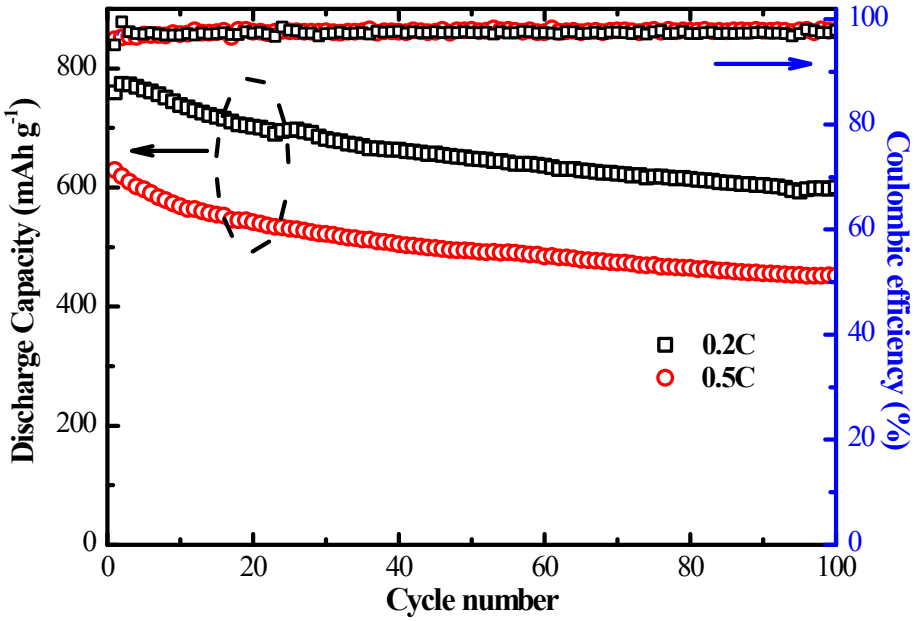

Fig. S11 Cycling performance of the g-C/S composite electrode with a high sulfur loading of about 5.5 mg cm^{-2}. The coulombic efficiencies are also shown.